Cooperative Motion Control Using Hybrid Acoustic-Optical Communication Networks

February 2021

Rodrigo Rego (rodrigorego@tecnico.ulisboa.pt)
Instituto Superior Técnico, Lisboa, Portugal

***Abstract*—There is currently widespread interest in the development of groups of autonomous underwater vehicles for ocean exploration. This calls for the deployment of robots that can act in cooperation by exchanging data over communication networks. For this purpose, acoustic networks have been so far the choice par excellence. However, for operations involving vehicles operating at close range, there is currently a flurry of activity on the use of optical-based communication systems, capable of higher transmission rates. As a result, the goal of this work is to make optical communications viable and to use both communication technologies during underwater cooperative missions. Motivated by this goal, the first part of this work proposes single vehicle motion control algorithms. Namely, an inner-loop heading controller that accepts references from an outer-loop path following controller designed at the kinematic level. Simulations with the MEDUSA-class vehicles illustrate the implementation of the proposed control systems, for different path following approaches. The second part of this work is dedicated to cooperative motion control issues. A coordination controller is designed and discrete communications among the vehicles are considered, taking into account the acoustic communications and triggering mechanisms that reflect their limitations. Lastly, the third part of the work proposes an algorithm to make optical communications viable, which ultimately boils down to achieving optical beam alignment between a pair of cooperative agents. The proposed algorithm is illustrated by simulation results that show optical beam alignment being reached for a pair of vehicles in a cooperative formation.**

Keywords: Motion Control, Path Following, Cooperative Control, Autonomous Underwater Vehicles

I. Introduction

Acoustic systems are the pervasive solution to communications, but their price is quite high and transmissions rates low. For this reason, there is currently considerable interest in the possible use of optical modems, as affordable units with the capability to transmit data at higher rates. Optical communication systems have, however, narrow directivity patterns, posing a challenge to achieve optical beam alignment while steering the vehicles.

As a result, the emphasis of this work lies in the development of algorithms for cooperative maneuvers, using data exchanged among the vehicles, by resorting to acoustic modems, when the vehicles are distant from each other and to broadcast their coordination states, and optical modems, when the vehicles operate at close range. In the latter case, the optical modems can also serve the dual purpose of transferring large volumes of data from one vehicle to another.

A. Topic Overview

The strategy to achieve single vehicle motion control starts with designing an inner-loop heading controller by state-feedback. In succession, an outer-loop for path following is designed, which will feed a reference to the inner-loop. This inner-outer loop decoupling strategy is commonly adopted as it offers flexibility. All of this is done considering a linearised system of the MEDUSA vehicle at a particular speed of operation, and designing a controller that is then applied, with proper modifications, to the original nonlinear system.

The adopted approach to achieve path following is based on the kinematics of the problem. Lyapunov's direct method is used to design an outer-loop path following controller by formulating appropriate control laws that make the Lyapunov function decrease. This method is explored by Micaelli and Samson in [1], having been improved by L. Lapierre in [2], in order to solve an initial condition constraint and to prove global convergence. The basic reasoning is to control explicitly the rate of progression of a "virtual target" to be tracked along the path, making the vehicle's path converge to the target's path.

Regarding cooperative motion control, a certain vehicle formation, during a cooperative mission, is achieved with a coordination controller that must be designed, which relies on a communication network scheme represented by a graph. This controller drives a certain coordination error to zero. It is important to consider [3] to address the consensus problem and look into [4] to establish and model discrete communications, which introduce the concept of triggering functions and allow the broadcast of the agents' coordination states to take place at discrete instants of time.

Lastly, having achieved single and multiple vehicle motion control, the optical beam alignment problem is addressed, between a pair of optical communication modems mounted on the vehicles. The proposed mechanism considers two phases: one where a rough alignment of the beams is reached, followed by another where a refinement is introduced. The reasoning behind the refinement phase is to apply a correction term that sweeps a neighborhood of the roughly determined alignment angles. These angles are computed by resorting to local information that each vehicle has access to, useful to determine

estimates of where the neighbor and vehicle itself are on top of the path that is being followed.

II. Autonomous Underwater Vehicle Model

This section presents the simplified model of an AUV for planar motion, with 3 degrees of freedom (DOF). Further simplifications are done taking into consideration the specifics of the MEDUSA class of autonomous underwater vehicles. This is an essential step towards designing and testing a controller for the system that we wish to control. This section is based on previous work, namely [5].

A. Notation

The pose of an AUV in 3D space can be completely described using six variables. These variables, and the two relevant reference frames, are shown in figure 1.

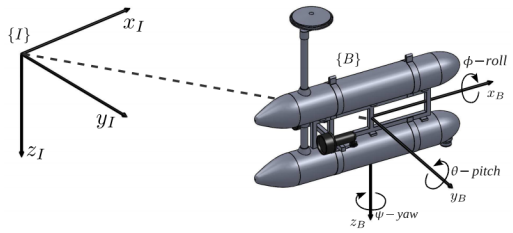

Fig. 1: AUV reference frames and notation. (source: [6])

The body-fixed reference frame is represented by $\{B\}$ and the inertial reference frame is represented by $\{I\}$. The body frame is fixed to the vehicle's centre of mass, with the principal axes of inertia coincident with the body axes x_B, y_B, z_B. With the inertial frame $\{I\}$ fixed somewhere in the world, it is possible to describe the pose of the vehicle relatively to this frame.

Now that the frames have been established, the definition of the notation used to express the pose of the vehicle, as well as its velocities, forces, and torques is as follows:

- position of $\{B\}$ expressed in $\{I\}$: $\boldsymbol{\eta}_1 = [x, y, z]^T$;
- orientation of $\{B\}$, in Euler-angles, with respect to $\{I\}$: $\boldsymbol{\eta}_2 = [\phi, \theta, \psi]^T$;
- linear velocity of $\{B\}$ with respect to $\{I\}$, expressed in $\{B\}$: $\boldsymbol{\nu}_1 = [u, v, w]^T$;
- angular velocity of $\{B\}$ with respect to $\{I\}$, expressed in $\{B\}$: $\boldsymbol{\nu}_2 = [p, q, r]^T$;
- forces acting on the vehicle, expressed in $\{B\}$: $\boldsymbol{\tau}_1 = [X, Y, Z]^T$;
- moments acting on the vehicle, expressed in $\{B\}$: $\boldsymbol{\tau}_2 = [K, M, N]^T$.

B. Simplified Kinematic Model

For a planar motion 3 DOF model, let $\boldsymbol{p} = [x, y]^T$ denote the inertial position vector and $\boldsymbol{v} = [u, v]^T$ denote the linear velocity vector, in the body-fixed coordinates, the kinematic model can be expressed as

$$\begin{cases} \dot{x} = u\cos(\psi) - v\sin(\psi) \\ \dot{y} = u\sin(\psi) + v\cos(\psi) \end{cases}. \tag{1}$$

In reality, the sway linear velocity v is expensive to measure. Usually, for the type of AUV to be used, v takes small values, therefore it can be neglected without affecting much the end results. As a result, this simplification yields the following model:

$$\begin{cases} \dot{x} = u\cos(\psi) \\ \dot{y} = u\sin(\psi) \end{cases}. \tag{2}$$

C. Simplified Dynamic Model

Likewise, regarding a 3 DOF simplification for planar motion, the dynamic model can be expressed as

$$\begin{aligned} &m_u\dot{u} - m_v vr + d_u u = \tau_u \\ &m_v\dot{v} + m_u ur + d_v v = \tau_v \\ &m_r\dot{r} - m_{uv}uv + d_r r = \tau_r \end{aligned}, \tag{3}$$

where the parameters that describe the dynamics are given by

$$\begin{aligned} m_u &= m - X_{\dot{u}} & d_u &= -X_u - X_{u|u|}|u| \\ m_v &= m - Y_{\dot{v}} & d_v &= -Y_v - Y_{uv|}|v| \\ m_r &= I_z - N_{\dot{r}} & d_r &= -N_r - N_{r|r|}|r| \\ m_{uv} &= m_u - m_v \end{aligned}. \tag{4}$$

This model can be further simplified if one desires to neglect the sway linear velocity, v, as well.

The next section will take into consideration the specifics of the MEDUSA class of autonomous underwater vehicles, to yield the final models for this specific type of vehicle.

D. MEDUSA-class Vehicles

The MEDUSA-class vehicles have two thrusters arranged symmetrically relatively to the xOz plane, with the direction of x. These thrusters can operate in common mode, moving the vehicle forward or backwards, or in differential mode, allowing the vehicle to turn around its z-axis. The diver version of the vehicles has two additional thrusters aligned with the z-axis, allowing for heave control.

Having described the MEDUSA-class vehicles' thrusters, it is possible to define

$$\begin{aligned} \tau_u &= F_s + F_p \\ \tau_r &= l\,(F_s - F_p)' \end{aligned} \tag{5}$$

where F_s and F_p are the force produced by the starboard thruster and the force produced by the portside thruster, respectively. Moreover, $l = 0.15$ m, for a MEDUSA vehicle. On top of this, there are no actuators to control the sway, this means that $\tau_v = 0$.

The most recent model parameters being used are defined in the following table:

$m = 17.0$ kg	$I_z = 1$ kg·m^2	
$X_{\dot{u}} = -20$ kg	$Y_{\dot{v}} = -30$ kg	$N_{\dot{r}} = -8.69$ kg·m^2
$X_u = -0.2$ kg/s	$Y_v = -50$ kg/s	$N_r = -4.14$ kg·m/s
$X_{\|u\|u} = -25$ kg/m	$Y_{\|v\|v} = -0.01$ kg/m	$N_{\|r\|r} = -6.23$ kg·m

TABLE I: Model parameters for the MEDUSA-class vehicle.

III. Heading Control

This section addresses the design of a heading controller for the vehicle. For this purpose, a state-space representation of the vehicle's model will be adopted, based on the previously obtained simplified models.

The system to be controlled is nonlinear. For this reason, a linearisation about an equilibrium point can be performed, in order to apply the Linear Quadratic Regulator (LQR) method to control the vehicle's heading using state feedback.

A. State-Space Model

Assuming that a system has n states, p inputs and q outputs, a state-space representation is given by

$$\begin{aligned}\dot{x}(t) &= Ax(t) + Bu(t)\\ y(t) &= Cx(t) + Du(t)\end{aligned}.$$

In this case, the state vector is given by $x = [v, r, \psi]^T$ ($n = 3$) and the input is $u = \tau_r$ ($p = 1$). Since the yaw angle is to be controlled, the output is $y = \psi$ ($q = 1$), assuming the notation simplification: $x(t) = x$, $u(t) = u$ and $y(t) = y$. Moreover, $A \in \mathbb{R}^{n\times n}$ is the state matrix, $B \in \mathbb{R}^{n\times p}$ is the input matrix, $C \in \mathbb{R}^{q\times n}$ is the output matrix and finally, in this case, the system doesn't have a direct feedthrough, so $D \in \mathbb{R}^{q\times p}$ is a zero matrix.

The linearisation is to be performed for a constant linear velocity of operation $u^* = 0.5$ m/s, $\bar{x} = [0, 0, 0]^T$, and the input $\bar{u} = 0$. This is a reasonable approximation because the side-slip and the rotation speeds are small with these vehicles.

By isolating the state variables and neglecting the sway linear velocity v, it is possible to obtain the following model

$$\begin{aligned}\dot{r} &= -\frac{d_r}{m_r}r + \frac{\tau_r}{m_r}.\\ \dot{\psi} &= r\end{aligned} \tag{6}$$

The linearisation is defined as

$$A = \left[\begin{array}{cc} \frac{\partial \dot{r}}{\partial r} & \frac{\partial \dot{r}}{\partial \psi} \\ \frac{\partial \dot{\psi}}{\partial r} & \frac{\partial \dot{\psi}}{\partial \psi} \end{array}\right]_{\substack{x=\bar{x}\\u=\bar{u}}} \qquad B = \left[\begin{array}{c} \frac{\partial \dot{r}}{\partial \tau_r} \\ \frac{\partial \dot{\psi}}{\partial \tau_r} \end{array}\right]_{\substack{x=\bar{x}\\u=\bar{u}}}. \tag{7}$$

The resultant state-space model is

$$\begin{aligned}\left[\begin{array}{c}\dot{r}\\ \dot{\psi}\end{array}\right] &= \left[\begin{array}{cc}\frac{N_r}{m_r} & 0\\ 1 & 0\end{array}\right]\left[\begin{array}{c} r\\ \psi\end{array}\right] + \left[\begin{array}{c}\frac{1}{m_r}\\ 0\end{array}\right]u(t)\\ y(t) &= \left[\begin{array}{cc} 0 & 1\end{array}\right]\left[\begin{array}{c} r\\ \psi\end{array}\right]\end{aligned}. \tag{8}$$

B. Linear Quadratic Regulator

The control objective is to find, among the class of admissible control laws, the one which minimizes the cost criterion

$$J = \int_{t=0}^{\infty}\Big[x(t)^T Q x(t) + u(t)^T R u(t)\Big]dt, \tag{9}$$

where $Q \in \mathbb{R}^{n\times n}$ penalises the state error and $R \in \mathbb{R}^{p\times p}$ penalises the control effort. To ensure that the control problem is well-posed, one has to verify that the pair (A, B) is stabilizable and the pair $(A, \sqrt{Q})$ is detectable. If $Q = C^T C$, for some matrix C, it is shown in [7] that $(A, \sqrt{Q})$ is detectable if and only if (A, C) is detectable, under the assumption that Q is a positive semi-definite matrix, thus having only one positive semi-definite square root [8, Theorem 7.2.6]. Considering $Q = C^T C$, the cost criterion penalises the energy of the state for a virtual output, given by $y = Cx$, as follows:

$$\begin{aligned}J &= \int_{t=0}^{\infty}\Big[y(t)^T y(t) + u(t)^T R u(t)\Big]dt\\ &= \int_{t=0}^{\infty}\Big[x(t)^T C^T C x(t) + u(t)^T R u(t)\Big]dt.\end{aligned} \tag{10}$$

If the detectability and stabilizability assumptions are verified, there exists a unique stabilizable solution to the LQR problem, given by the state feedback control:

$$u(t) = -Kx(t), \tag{11}$$

where the gain vector $K \in \mathbb{R}^{n\times 1}$ satisfies

$$K = R^{-1}B^T P, \tag{12}$$

and $P \geq 0$ is a unique solution to the continuous time Algebraic Ricatti Equation:

$$A^T P + PA - PBR^{-1}B^T P + Q = 0, \tag{13}$$

which is used to solve the LQR optimal control problem.

The challenge of designing a LQR controller lies in finding appropriate weighting matrices Q and R. This implies an iterative process of weight tuning. A first good iteration for the Q matrix is given by the Bryson's rule, where the Q weights are initially set with the inverse of the maximum accepted value of the square of each state variable, denoted x^2_{max}.

This concludes the definition of the state feedback control law $u(t) = -Kx(t)$.

C. Integral Effect and Anti-Windup

To complete the design of the heading controller, an integral effect can be added in order to reject constant disturbances (constant external inputs affecting the command of the thrusters). To achieve this, one has to consider an additional integrator placed before the disturbance, thus, integrating the error with respect to time.

Adding this effect implies the addition of ϵ to the state vector, as a state variable with a corresponding gain in the K vector. The previous state-space model is, therefore, adapted taking into account the dynamics of ϵ, given by $\dot{\epsilon} = \psi_{ref} - \psi$.

The block diagram of the controlled system with integral effect is shown in figure 2.

It is important to adopt an anti-windup design that stops integrating the error once the input saturates. The anti-windup scheme should prevent the divergence of the integral error when the control cannot keep up with the reference, maintaining the integral errors "small" (avoids error buildup), defined as

$$u_{aw} = \int K_\epsilon\left[e + K_{aw}(\mathrm{sat}(u) - u)\right]dt. \tag{14}$$

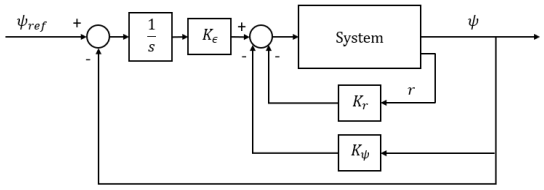

Fig. 2: Block diagram of the controlled system with integral effect.

The issue now is that, for the anti-windup scheme to be implemented and produce a quick action, the integrator must be right next to the plant. More importantly, placing the integrator next to the plant results in a Bumpless Transfer method.

In order to accomplish this, one can look into the theory presented in the paper [9]. This paper proves that it is possible to place the integrator after the state feedback through the gain vector K, by first differentiating the state, while preserving the closed-loop eigenvalues as well as the input-output properties of the original linear closed-loop system locally. Therefore, the new configuration represented in figure 3 is proven possible.

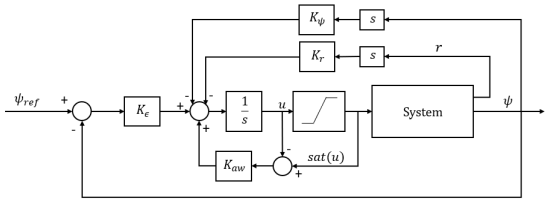

Fig. 3: Anti-windup design with integral effect next to the plant.

IV. Path Following

This section addresses the design of an outer-loop that can generate yaw angle references knowing the path and making use of the vehicle kinematics. The goal is to make the vehicle converge to and follow the path at a desired speed, that can be path dependent.

This suggests that an inner-outer loop decoupling strategy be implemented in order to control the motion of a single vehicle, designing an outer-loop path following controller based on the vehicle kinematics.

A. Outer-Loop Control

The proposed path following approach uses Lyapunov's direct method to design the outer-loop path following controller. This is done by proposing the virtual control laws that make the Lyapunov function decrease, also proving stability.

This approach is originally tackled by Micaelli and Samson in [1], however, only local convergence of the vehicle's path to the desired one is proven, due to a stringent initial condition constraint. L. Lapierre et al. [2] improves upon the previous work, by controlling explicitly the rate of progression of a "virtual target" to be tracked along the path, making the vehicle's path converge to the target's and resorting to a Serret-Frenet frame.

The path following configuration is represented in figure 4. The position of the vehicle is represented by the centre of mass $\boldsymbol{M}$, with coordinates $[s_1, y_1]^T$ in the frame $\{T\}$, and $[X, Y]^T$ in the fixed inertial frame $\{I\}$. The signed curvilinear abscissa of $\boldsymbol{P}$ along the path is denoted s, which is associated with the Serret-Frenet frame $\{T\}$.

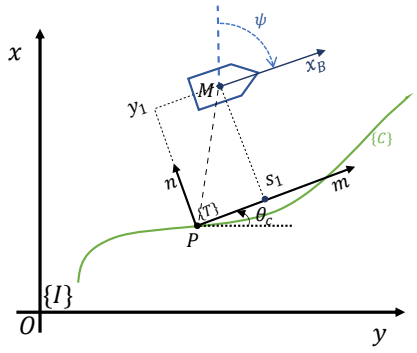

Fig. 4: Configuration for the L. Lapierre's guidance method.

Let the rotation matrix from $\{I\}$ to $\{T\}$ be expressed as

$$R_I^T\left(\frac{\pi}{2}-\beta\right)=\begin{bmatrix}\sin\left(\frac{\pi}{2}-\beta\right) & \cos\left(\frac{\pi}{2}-\beta\right) & 0\\ \cos\left(\frac{\pi}{2}-\beta\right) & -\sin\left(\frac{\pi}{2}-\beta\right) & 0\\ 0 & 0 & 1\end{bmatrix}, \tag{15}$$

parametrized locally by the angle β, considering that $\theta_c = \pi/2 - \beta$. A classical law of mechanics gives

$$\left[\frac{d\overrightarrow{OM}}{dt}\right]_I=\left[\frac{d\overrightarrow{OP}}{dt}\right]_I+\left[\frac{d\overrightarrow{PM}}{dt}\right]_T+(\overrightarrow{w_c}\times\overrightarrow{PM}), \tag{16}$$

with

$$[\overrightarrow{\mathrm{OM}}]_I=\begin{bmatrix}X\\Y\\0\end{bmatrix},\quad [\overrightarrow{\mathrm{OP}}]_I=\begin{bmatrix}s\\0\\0\end{bmatrix},\quad [\overrightarrow{\mathrm{PM}}]_T=\begin{bmatrix}s_1\\y_1\\0\end{bmatrix}, \tag{17}$$

and

$$\vec{w}_c\times\overrightarrow{PM}=\begin{bmatrix}0\\0\\\dot\beta=c_c(s)\dot s\end{bmatrix}\times\begin{bmatrix}s_1\\y_1\\0\end{bmatrix}=\begin{bmatrix}-c_c(s)\dot s y_1\\c_s(s)\dot s s_1\\0\end{bmatrix}, \tag{18}$$

where $[\vec{w}_c]_I$ is the rotation velocity vector of frame $\{T\}$ with respect to $\{I\}$ and $c_c(s)$ is the path's curvature at $\{T\}$, one gets

$$R_I^T\left(\frac{\pi}{2}-\beta\right)\begin{bmatrix}\dot X\\\dot Y\\0\end{bmatrix}=\begin{bmatrix}\dot s\left[1-c_c(s)y_1\right]+\dot s_1\\\dot y_1+c_c(s)\dot s s_1\\0\end{bmatrix}. \tag{19}$$

Solving for $\dot{s_1}$ and $\dot{y_1}$, recalling the simplified kinematic model of the vehicle and introducing the variable $\theta = \psi - \beta$, yields the kinematic model of the vehicle in the (s_1, y_1) coordinates given by

$$\begin{cases} \dot{s}_1 = -\dot{s}\,(1 - c_c y_1) + u\cos(\theta) \\ \dot{y}_1 = -c_c \dot{s} s_1 - u\sin(\theta) \\ \dot{\theta} = r - c_c \dot{s} \end{cases}, \tag{20}$$

where $r = \dot{\psi}$.

The outer-loop control objective is to ultimately drive θ to zero, so that the vehicle orients itself with the trajectory, and to drive the cross-track error y_1 to zero, so that the vehicle converges to the path.

Using a nonlinear controller design strategy based on the kinematic model, the control objectives can be embodied in a Lyapunov candidate function

$$V_1 = \frac{1}{2}\left(s_1^2 + y_1^2\right) + \frac{1}{2\gamma}\left(\theta - \delta\left(y_1, u\right)\right)^2, \tag{21}$$

where it is assumed that
A.1: $\delta(0, u) = 0$.
A.2: $y_1 u \sin\delta\left(y_1, u\right) \geq 0, \forall y \forall u$.
A.3: $\lim_{t\to\infty} u(t) \neq 0$.

Letting the ideal kinematic control laws for s and θ, given by the authors of [2], be defined as

$$\begin{array}{l} \dot{s} = u\cos\theta + k_1 s_1 \\ \dot{\theta} = \dot{\delta} + \gamma y_1 u \frac{\sin\theta - \sin\delta}{\theta - \delta} - k_2(\theta - \delta) \end{array}, \tag{22}$$

where k_1 and k_2 are positive gains. Then,

$$\dot{V}_1 = -k_1 s_1^2 - y_1 u \sin\delta - k_2 \frac{(\theta - \delta)^2}{\gamma} \leq 0, \tag{23}$$

where the second term, $y_1 u \sin\delta$, respects the inequality through assumption A.2. As a result, these control laws can be used to achieve the convergence of the vehicle to the path at a desired speed, hence accomplishing path following.

Given that ultimately the vehicle is steered by receiving values of $r = \dot{\psi}$ and recalling (20),

$$\begin{aligned} r &= \dot{\theta} + c_c \dot{s} \\ &= \dot{\delta} + \gamma y_1 u \frac{\sin\theta - \sin\delta}{\theta - \delta} - k_2(\theta - \delta) + c_c \dot{s}. \end{aligned} \tag{24}$$

The choice of the $\delta(y_1, u)$ function is instrumental in shaping the transient manoeuvrers during the path approach phase. Looking again into the references [1] and [2], it is recommended the usage of

$$\delta\left(y_1, u\right) = \theta_a \tanh\left(k_\delta y_1 u\right), \tag{25}$$

where $0 < \theta_a < \pi/2$, k_δ is an arbitrary positive gain and $\delta(y_1, u)$ is differentiable with respect to u at $u = 0$.

With properly defined path parametrization, one can obtain measures of (s_1, y_1), $c_c(s)$ and θ_c (or $\beta = \pi/2 - \theta_c$) to the aforementioned virtual control laws and achieve path following.

B. Path Following with Ocean Currents

The previous path following approach gives yaw rate, r, references to the inner-loop, instead of yaw angle, ψ, references. If ocean currents are to be taken into consideration, the previous outer-loop control laws must be adapted to both consider the ocean currents and to output yaw angle ψ references.

The reasoning behind the approach to deal with the ocean current disturbance is to feed compensated heading control references that are meant to align the total velocity vector of the vehicle with the trajectory, instead of the vehicle's main body axis. To achieve this, a current observer, in the fixed inertial frame, is used so that it is possible to then compensate the heading references with the intent of canceling the perpendicular component of the velocity of the current to the trajectory.

Firstly, it is important to consider the velocity notation:

- $\boldsymbol{V_c}$ – velocity vector of the ocean current;
- $V_c^{\parallel}$ – parallel component of the ocean current to the trajectory;
- $V_c^{\perp}$ – perpendicular component of the ocean current to the trajectory.

The total velocity vector of the vehicle is denoted by $\boldsymbol{V_T}$, the goal being to align this velocity vector with the trajectory, which causes an angle mismatch, σ, relatively to the vehicle's heading – course angle. The linear velocity of the vehicle is depicted by u, the vessel's velocity relatively to the water.

Recalling the L. Lapierre's kinematic model and taking the ocean currents into account, the new kinematic model is given by

$$\begin{cases} \dot{s}_1 = -\dot{s}\,(1 - c_c y_1) + u\cos(\theta) + V_c^{\parallel} \\ \dot{y}_1 = -c_c \dot{s} s_1 - u\sin(\theta) + V_c^{\perp} \end{cases}. \tag{26}$$

Using a new Lyapunov function

$$V_1 = \frac{1}{2}\left(s_1^2 + y_1^2\right), \tag{27}$$

the ideal kinematic control laws for s and θ are now given by

$$\begin{array}{l} \dot{s} = u\cos\theta + k_1 s_1 + V_c^{\parallel} \\ \theta = \arcsin\left[\mathrm{sat}\left(k_2 y_1 + \frac{V_c^{\perp}}{u}\right)\right] \end{array}, \tag{28}$$

where k_1 and k_2 are positive gains and u is set to be constant and positive. Therefore,

$$\dot{V}_1 = -k_1 s_1^2 - u k_2 y_1^2 \leq 0, \tag{29}$$

proving that the chosen virtual control law for θ will make the cross-track error converge to zero, as intended. Recalling that $\theta = \psi - \beta$,

$$\psi = \arcsin\left[\mathrm{sat}\left(k_2 y_1 + \frac{V_c^{\perp}}{u}\right)\right] + \beta\ . \tag{30}$$

As a result, the L. Lapierre's path following method is now defined to give yaw references to the inner-loop, ψ_{ref}, while taking into account the ocean currents.

Following the same reasoning as in [10] and looking at the filter theory contemplated in [11], it is possible to propose an observer to estimate the ocean current disturbance, assuming that a position system is available to provide measurements of the position of the vehicle, $\boldsymbol{p} = [x, y]^T$. Moreover, since the influence of the ocean currents is not a major topic of this work, it is also assumed that the vehicle's speed relatively to the fluid, u, is measured by a **DVL** (Doppler Velocity Log).

The structure of the observer, fixed in the world frame $\{I\}$, is based on the vehicle kinematics, ignoring the sway speed v,

$$\begin{cases} \dot{x} = u\cos(\psi) + v_{c_x} \\ \dot{y} = u\sin(\psi) + v_{c_y} \end{cases}, \tag{31}$$

where v_{c_x} and v_{c_y} denote the components of the ocean current disturbance in $\{I\}$.

Taking into account the measured quantities, the kinematic model and defining the notation $\hat{x}$ as an estimate of the inertial x and $\tilde{x} := x - \hat{x}$ as the error of the estimate (the same notation is used for y and v_{c_i}), an observer for the component v_{c_x} is

$$\begin{cases} \dot{\hat{x}} = u\cos\psi + \hat{v}_{c_x} + k_{x_1}\tilde{x} \\ \dot{\hat{v}}_{c_x} = k_{x_2}\tilde{x} \end{cases}. \tag{32}$$

Clearly, the estimate errors $\tilde{x}$ and $\tilde{v}_{c_x}$ are asymptotically exponentially stable if all the roots of the characteristic polynomial $p(s) = s^2 + k_{x_1}s + k_{x_2}$ associated with the system

$$\begin{bmatrix} \dot{\tilde{x}} \\ \dot{\tilde{v}}_{c_x} \end{bmatrix} = \begin{bmatrix} -k_{x_1} & 1 \\ -k_{x_2} & 0 \end{bmatrix} \begin{bmatrix} \tilde{x} \\ \tilde{v}_{c_x} \end{bmatrix} \tag{33}$$

have strictly negative real parts.

The observer for the component v_{c_y} can be written in an analogous manner, to yield

$$\begin{cases} \dot{\hat{y}} = u\sin\psi + \hat{v}_{c_y} + k_{y_1}\tilde{y} \\ \dot{\hat{v}}_{c_y} = k_{y_2}\tilde{y} \end{cases}. \tag{34}$$

The estimate errors $\tilde{y}$ and $\tilde{v}_{c_y}$ are similarly proven asymptotically exponentially stable, as the previous situation.

To obtain the perpendicular and parallel velocity components in the Serret-Frenet frame one should recall the transformation $R_I^T(\theta_c)$ applied to $[v_{c_x}, v_{c_y}, 0]^T$.

As a result, it is now possible to estimate the ocean current disturbance, which is, in turn, used to compensate the heading so that the total velocity vector of the vehicle is aligned with the trajectory.

V. Multiple Vehicle Coordination Control

Coordination control between a group of vehicles is to be achieved through the design of a coordination controller that drives a certain coordination error to zero, reaching consensus among the vehicles' states.

It is important to consider that the agents must broadcast their coordination states to their neighbors. For this reason, the communication network scheme is represented by an undirected graph $\mathcal{G} = (\mathcal{V}, \mathcal{E})$ such that elements of $\mathcal{E}$ consist of two elements from $\mathcal{V}$, i.e. $\mathcal{E} \subseteq [\mathcal{V}]^2$. The elements of $\mathcal{V}$ are called vertices, or nodes of $\mathcal{G}$ and the elements $\mathcal{E}$ are its edges, or links. One edge connects two nodes.

Additionally, discrete communications must be taken into consideration, in order to reflect the communication modems limitations and common operation. As a result, a mechanism in which the vehicles only need to exchange data with their neighbors when necessary, in accordance with an appropriately defined criterion will be proposed, introducing the concept of triggering functions.

A. Graph Theory

In the multiple vehicle coordination control scenario, the graph edges represent the communication link between a pair of vehicles, which are undirected, allowing for communications in both directions: from node n_0 to n_1 and from n_1 to n_0 (each node represents a vehicle), for example.

Additionally, $\mathcal{N}^{[i]}$ represents the set of neighboring nodes of node i with which this node communicates.

In this context, two main definitions are relevant: the adjacency matrix and the degree matrix.

Definition 1 (Adjacency Matrix)**.** *The adjacency matrix $A = (a_{ij})_{N\times N}$ of $\mathcal{G}$ in which its elements are defined as*

$$a_{ij} := \begin{cases} 1 & \text{if } n_i n_j \in \mathcal{E} \\ 0 & \text{otherwise} \end{cases}. \tag{35}$$

Definition 2 (Degree Matrix)**.** *Let $\mathcal{G}$ be a graph. The degree matrix, $D = (d_{ij})_{N\times N}$ of $\mathcal{G}$ can have each element of the matrix defined as*

$$d_{ij} := \begin{cases} d(n_i) = \left|\mathcal{N}^{[i]}\right| & \text{if } i = j \\ 0 & \text{otherwise} \end{cases}. \tag{36}$$

From the two latter definitions, it is possible to define the Laplacian, L, of the undirected graph to represent it. The expression of the Laplacian of an undirected graph is defined as $L = D - A$. It is well known that if $\mathcal{G}$ is undirected, then L is symmetric and $L\mathbf{1} = \mathbf{0}$, where $\mathbf{1} := [1]_{N\times 1}$ and $\mathbf{0} := [0]_{N\times 1}$, with N being the total number of nodes.

One last modification can be made to the Laplacian form of a graph to obtain the normalized Laplacian

$$L_D = D^{-1}(D - A). \tag{37}$$

B. Coordination Control

The coordination problem statement, referring to [12], can be formally defined as

Problem 1 (Coordination Problem)**.** *For vehicle $i = 1, \ldots, n$ derive a control law for $\dot{\gamma}^{[i]}$ as a function of local states and the variables $\gamma^{[j]}, j \in \mathcal{N}^{[i]}$ such that $\gamma^{[i]} - \gamma^{[j]}, \forall i, j$ approach a small neighborhood of zero as $t \to \infty$ and the formation travels at the speed $u_d(t)$, that is, $\dot{\gamma}^{[i]} \to u_d \forall i$.*

With the stated coordination problem, it is important to define the coordination state $\gamma^{[i]}$, which corresponds to the normalized arc-length, computed from the outer-loop.

The distributed coordination controllers, designed to make $\gamma^{[i]}$ reach consensus, will yield a correction term, $u_c^{[i]}$, that is added to the desired speed of each vehicle, with the goal of

driving the coordination error to zero. Thus, the desired speed that enters the inner-loop is

$$u_d^{[i]} = u_L^{[i]} + u_c^{[i]}. \tag{38}$$

Knowing that the communication network is modeled by an undirected graph, the previously defined normalized Laplacian, L_D, can be used to help define the coordination error vector:

$$\boldsymbol{\xi} = L_D \boldsymbol{\gamma}, \tag{39}$$

where $\boldsymbol{\xi}$ is the coordination error vector and $\boldsymbol{\gamma} = [\gamma^{[1]}, ..., \gamma^{[N]}]^T$ is the state vector containing the coordination state of each vehicle.

Assuming, for now, continuous communications, a distributed control law for $\boldsymbol{u_c}$ that drives ξ_i to zero is given by

$$\boldsymbol{u_c} = -k_\xi \tanh\left(L_D \boldsymbol{\gamma}\right), \tag{40}$$

where k_ξ is a positive constant and the hyperbolic tangent is used to bound $\boldsymbol{u_c}$, in order to prevent the speed reference from becoming negative.

As a result, it is possible now to use the defined distributed control law to reach consensus, thus achieving coordination. Moving forward, one should then take into account the discrete communications among vehicles.

C. Event-Triggered Communication Mechanism

An Event-Triggered Communication (ETC) mechanism is proposed, in which the vehicles only need to exchange data with their neighbors when necessary, in accordance with a properly defined triggering function that contains all the local information that vehicle i has at a certain instant of time (referring to [3] and [4]).

In this mechanism, instead of using the true neighboring states, $\gamma^{[j]}; j \in \mathcal{N}^{[i]}$, the previously defined control law (40) uses their estimates – if any agent can produce good estimates of the neighboring states, then there is no need to communicate continuously. Letting $\hat{\gamma}^{[ij]}$ be an estimate of $\gamma^{[j]}$ computed by vehicle i and $\hat{\gamma}^{[i]}$ is an estimate of the vehicle's state itself, the ETC control law is given by

$$u_c^{[i]} = -k_\xi \tanh\left(\hat{\gamma}^{[i]} - \frac{1}{\left|\mathcal{N}^{[i]}\right|} \sum_{j \in \mathcal{N}^{[i]}} \hat{\gamma}^{[ij]}\right); i \in \mathcal{N}. \tag{41}$$

Letting $\left\{t_k^{[i]}\right\}; k \in \mathbb{N}$ be the sequence of time instants at which vehicle i sends its current value of $\gamma^{[i]}(t_k^{[i]})$ to its neighbors, during the interval $\mathcal{T}_k^{[i]} := \left[t_k^{[i]}, t_{k+1}^{[i]}\right)$ and for $t \in \mathcal{T}_k^{[i]}$, an estimator for $\hat{\gamma}^{[i]}$ can be defined as

$$\begin{aligned} \dot{\hat{\gamma}}^{[i]}(t) &= \bar{u}_L^{[i]} \\ \hat{\gamma}^{[i]}\left(t_k^{[i]}\right) &= \gamma^{[i]}\left(t_k^{[i]}\right), \end{aligned} \tag{42}$$

knowing that the state is the normalized arc-length, then $\bar{u}_L^{[i]}$ corresponds to the normalized desired speed given by the path generation block. The second equation implies that whenever vehicle i broadcasts $\gamma^{[i]}$ to its neighbors, the initial condition for $\hat{\gamma}^{[i]}$ will be reset. The estimator for $\hat{\gamma}^{[ji]}$ is obtained analogously.

Having defined the new distributed control law, which considers the estimates of the states, the next step is to define the triggering function that dictates when should there be a state broadcast.

D. Time-Dependent Triggering Events

For a purely time-dependent triggering event, to ensure that the estimation error is bounded, vehicle i should transmit $\gamma^{[i]}$ whenever $e^{[i]}$ hits a designed threshold $\eta^{[i]}$ that is dependent on time, where $e^{[i]}(t) = \hat{\gamma}^{[i]}(t) - \gamma^{[i]}(t)$ is the local estimation error of vehicle i itself. The triggering function for vehicle i is given by

$$h^{[i]}(t) = \left|e^{[i]}(t)\right| - \eta^{[i]}(t), \tag{43}$$

where $\eta^{[i]}(t)$ belongs to a class of non-negative functions $\mathcal{C}$ defined by $\mathcal{C} := \{f : R_{\geq 0} \to R_{\geq 0} \mid\leq\ 0 \leq f(t) \leq c_u\}$ for all $i \in \mathcal{N}$. For example, $\eta^{[i]}(t) = c_1 + c_2 e^{-\alpha t}$ with a proper choice of c_1, c_2 and α is a typical function belonging to $\mathcal{C}$. With this definition, vehicle i will send its state to its neighbors whenever $h^{[i]}(t) \geq 0$.

E. State-Dependent Triggering Events

Regarding state-dependent triggering events, it is possible to introduce another triggering function for each vehicle that depends on the information about its state estimate and the state estimates of the neighboring vehicles that communicate with it.

With the local information of the states, a new threshold is defined for $(e^{[i]})^2(t)$, resulting in the following triggering function:

$$h^{[i]}(t) = (e^{[i]})^2(t) - \left(\theta^{[i]} \frac{\sigma}{\sigma^{[i]}} \sum_{j \in \mathcal{N}^{[i]}} a_{ij} \left(\hat{\gamma}^{[i]}(t) - \hat{\gamma}^{[ij]}(t)\right)^2 + \epsilon_0\right), \tag{44}$$

where a_{ij} represents the adjacency matrix A entries, which take the value of 1 or 0. The other constants: $\sigma, \sigma^{[i]}, \theta^{[i]}$, and ϵ_0 are defined in [4] and, for the sake of simplicity, were deemed not relevant to show here. Likewise, with the above definition, vehicle i will send its state to its neighbors whenever $h^{[i]}(t) \geq 0$.

VI. Hybrid Network – Optical Communications

Optical communications have narrow directivity patterns, which make the issue challenging when they're added on moving agents, whose speeds are consistently being corrected in order to reach consensus. With this in mind, the major goal of this section is to accomplish optical beam alignment between a pair of vehicles. Each vehicle should be able to estimate the position of the neighbors on top of the path they are following, based on the information given by the

coordination states, and it is assumed that the optical modems have an independent rotation axis.

Beam alignment is planned to be accomplished with two phases: rough and refined alignment phases. Rough alignment aims to rotate the beams based on estimates of the positions of each vehicle, which may not lead to proper alignment due to the errors of the estimates. Refined alignment aims to apply small deviations to the rough alignment angle until the beams align, locking that beam orientation.

A. Rough Alignment Phase

Let $\boldsymbol{p_t} = [x_t, y_t]^T$ denote the position of the center of mass of the transmitting vehicle, with a_t denoting the central axis of the transmitting beam and α denoting the angle at which the transmitting beam is oriented. Likewise, let $\boldsymbol{p_r} = [x_r, y_r]^T$ denote the position of the center of mass of the receiving vehicle, with a_r denoting the central axis of the receiving beam, with orientation given by σ. Figure 5 represents the geometry of the beam alignment problem.

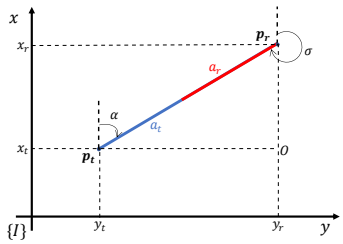

Fig. 5: Geometric representation of the optical beam alignment problem.

For now, it is assumed that each vehicle knows exactly $\boldsymbol{p_t}$ and $\boldsymbol{p_r}$ (and not their estimates). With the goal of overlapping a_t and a_r, a geometric analysis of the situation represented in 5 yields the following equations for α:

$$\alpha = \begin{cases} \frac{\pi}{2} - \arcsin(k), & y_r \geq y_t \\ -\frac{\pi}{2} + \arcsin(k), & y_r < y_t \end{cases}, \tag{45}$$

where k is given by

$$k = \frac{\mathrm{d}(\boldsymbol{O}, \boldsymbol{p_r})}{\|\boldsymbol{p_r} - \boldsymbol{p_t}\|}. \tag{46}$$

The numerator $\mathrm{d}(\boldsymbol{O}, \boldsymbol{p_r})$ denotes the signed distance between $\boldsymbol{O}$ and $\boldsymbol{p_r}$. As a result,

$$k = \frac{x_r - x_t}{\sqrt{(y_r - y_t)^2 + (x_r - x_t)^2}}. \tag{47}$$

Similarly, the equations for σ are defined as

$$\sigma = \begin{cases} \frac{3\pi}{2} - \arcsin(k), & y_r \geq y_t \\ \frac{\pi}{2} + \arcsin(k), & y_r < y_t \end{cases}. \tag{48}$$

In reality, each vehicle has local information about their own estimated coordination state and the estimated states of the neighboring vehicles. As a result, one has to compute $\boldsymbol{p_t}^{[i]}$ and $\boldsymbol{p_r}^{[ij]}$ using $\hat{\gamma}^{[i]}(t)$ and $\hat{\gamma}^{[ij]}(t)$, both for each vehicle of the pair, based on the path parametrization.

B. Refined Alignment Phase

A refinement is needed because, under uncertainty, one vehicle may have a wrong idea of the position of its neighbor during a period of time, requiring a small correction to the rough orientations.

The correction term applied to α and σ will work as a sweeping mechanism: sweeping a small neighborhood of each roughly determined angle until the beams align, locking that corrected orientation.

Letting α_c and σ_c denote the corrected angles, defined as

$$\begin{aligned} \alpha_c &= \alpha + A\sin(2\pi f_\alpha) \\ \sigma_c &= \sigma + A\sin(2\pi f_\sigma), \end{aligned} \tag{49}$$

where f_α and f_σ denote the oscillation frequencies of the correction term in hertz and A denotes the amplitude of the oscillations in degrees, one is capable of sweeping, having used a sine wave with a certain frequency and amplitude as a sweeping term.

One way of determining that refinement has reached its goal and that it was able to correct the orientation is by inspecting the power of the received signal. The power of the signal is largely impacted by how misaligned are the optical beams. The power variation is represented in figure 6.

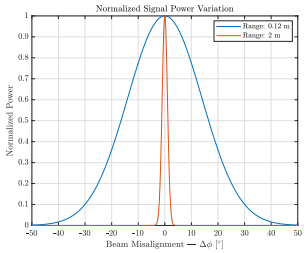

Fig. 6: Variation of the received signal power with the beam misalignment for two different ranges.

In a simulation environment, it is possible to have access to information that in reality each vehicle doesn't have. This is used to compute the ideal orientation for each beam and to evaluate how misaligned the beams are, $\Delta\phi$, during the rough alignment phase. From this, the refinement phase should be activated until the corrected orientation makes the received power be within a user defined threshold.

The following regards should be taken into account:

- The sweeping frequencies should be set according to $f_\alpha = 2f_\sigma$, increasing the chances of beam alignment per period of the sweeping signal with the smallest frequency.
- The amplitude of the sweeping oscillations should start small and then it should increase if, for every two periods of sweeping, beam alignment is not achieved, avoiding situations where small sweepings are not enough.

VII. Results

Considering coordination control, simulations were done taking into account a group of three vehicles in an in-line formation. Each vehicle has an inner-loop heading controller

and an outer-loop path following controller as described previously.

The adopted communication scheme is mathematically represented by the following Laplacian matrix

$$L = \begin{bmatrix} 1 & -1 & 0 \\ -1 & 2 & -1 \\ 0 & -1 & 1 \end{bmatrix}. \tag{50}$$

Figure 7 the cooperative mission being achieved with time-dependent ETC. Moreover, it is possible to observe when each vehicle transmits its state, based on the time-dependent triggering function.

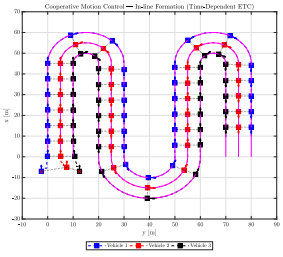

(a) Coordination of an in-line formation.

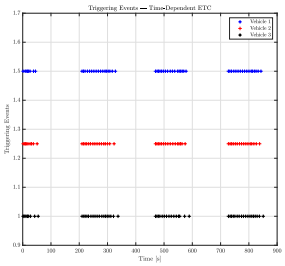

(b) Time-dependent triggering events over time.

Fig. 7: Cooperative motion control simulation of a group of three vehicles using time-dependent ETC.

As it is shown, considering that each vehicle estimates the state of its neighbors, the agents don't need to be communicating continuously to achieve coordination. Additionally, using a triggering function avoids communication congestion when one considers that underwater acoustic communications have slow data transference.

Better results seem to be obtained using state-dependent ETC, figure 8, which may be related to the fact that the triggering function uses more local information. These translate to more triggering during the transitions between path segments, which is ideal. The state errors, $\tilde{\gamma}_{ij}$, represented in figure 9 show that the states are synchronized asymptotically.

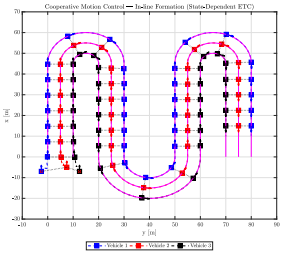

(a) Coordination of an in-line formation.

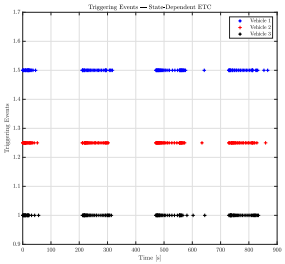

(b) State-dependent triggering events over time.

Fig. 8: Cooperative motion control simulation of a group of three vehicles using state-dependent ETC.

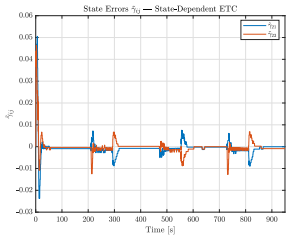

(a) State errors $\tilde{\gamma}_{ij}$.

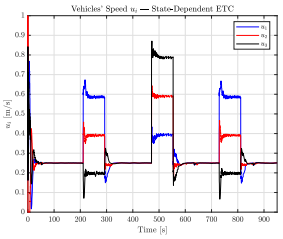

(b) Vehicles' speed u_i.

Fig. 9: Evolution of the state errors and the surge speed of each vehicle using state-dependent ETC.

These results for cooperative missions also show that the proposed inner and outer loops work properly, allowing each vehicle to be steered while following a desired path.

Regarding the proposed mechanism for optical beam alignment between a pair of vehicles, figure 10 shows the central axis of each beam reaching alignment during a cooperative mission.

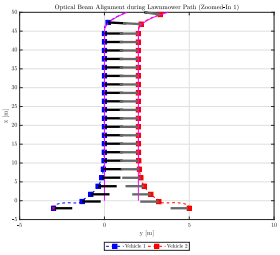

(a) Zoomed-in portion of the path 1.

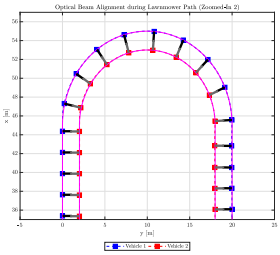

(b) Zoomed-in portion of the path 2.

Fig. 10: Optical beam alignment for a lawnmower path zoomed-in portions.

Most of the time, the rough alignment phase already produces a good enough orientation of the beams and only a small sweeping is required, as expected, observing figure 11. Nevertheless, the refinement phase makes the alignment error be more constrained to a neighborhood of zero.

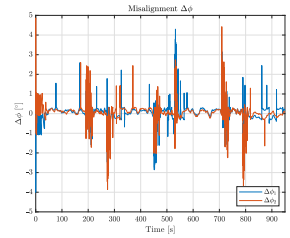

(a) Evolution of the misalignment $\Delta\phi$.

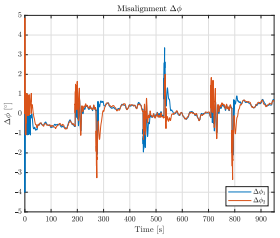

(b) Evolution of the misalignment $\Delta\phi$ without refinement.

Fig. 11: Evolution of the misalignment $\Delta\phi$ with and without refinement.

However, due to the range of communication (2 meters), the

power curve is very narrow, as represented before in figure 6, even a small deviation can produce a dramatic impact on the value of the received signal power, which is why, in figure 12, the normalized power shows sudden drops. Nevertheless, looking at the average and median values, most of the time, optical communications aim to be within the user defined power threshold.

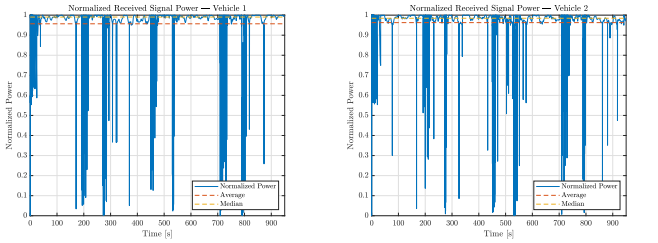

(a) Evolution of the received signal power of vehicle 1.

(b) Evolution of the received signal power of vehicle 2.

Fig. 12: Evolution of the received signal powers (lawnmower path + discrete communications).

These results show that optical communications can be a viable communication solution for underwater cooperative missions, hence proving that the proposed mechanism works properly. While the refined alignment is being reached, some communication intermittency is to be expected.

VIII. Conclusions

The purpose of this work was to ultimately show that using a hybrid communication network, during cooperative missions, is viable. Acoustic communications are commonly used with underwater autonomous vehicles to broadcast the state of the vehicles. However, optical communication modems are just now breaking through in this field and so the problems regarding their narrow directivity patterns boil down to reaching optical beam alignment between a pair of vehicles, which has been shown to be viable.

Nevertheless, due to the complexity of this optical beam alignment problem using moving cooperative agents, some communication intermittency is to be expected, still the proposed algorithm may just be enough to transmit mission data (such as maps and images) among the vehicles using the faster optical communications pillar of the hybrid network.

At the first stage, single and multiple vehicle motion control had to be achieved, considering coordination with discrete communications among the vehicles. This was essential to ultimately address the optical communications problem.

The major contribution was the proposal of the alignment mechanism, which resorts to two stages: a rough beam alignment phase followed by a refined one, which basically boiled down to implementing a sweeping mechanism until the optical beams overlapped.

As for future work, it would be important to test the beam alignment algorithm in real vehicles performing real cooperative missions, recalling that ocean currents have to be considered as studied in this work as well. Moreover, if this optical beam alignment algorithm shows promising results in real tests, then one could consider using the optical communications to transmit the vehicles' coordination states as well.

References

[1] Alain Micaelli and Claude Samson. Trajectory tracking for unicycle-type and two-steering-wheels mobile robots. *Rapports de recherche - INRIA*, (RR-2097), 1993.

[2] L. Lapierre, D. Soetanto, and A. Pascoal. Nonsingular path following control of a unicycle in the presence of parametric modelling uncertainties. *International Journal of Robust and Nonlinear Control*, 16(10):485–503, 2006.

[3] Nguyen T. Hung, Antonio M. Pascoal, and Tor A. Johansen. Cooperative path following of constrained autonomous vehicles with model predictive control and event-triggered communications. *International Journal of Robust and Nonlinear Control*, 30(7):2644–2670, 2020.

[4] N. T. Hung, F. C. Rego, and A. M. Pascoal. Event-triggered communications for the synchronization of nonlinear multi agent systems on weight-balanced digraphs. In *2019 18th European Control Conference (ECC)*, pages 2713–2718, 2019.

[5] Guilherme Manuel Vilela Sanches. Sensor-based formation control of autonomous marine robots. Master's thesis, Instituto Superior Técnico, 2015.

[6] Jorge Ribeiro. Motion control of single and multiple autonomous marine vehicles. Master's thesis, Instituto Superior Técnico, 2011.

[7] B.D.O. Anderson and J.B. Moore. *Optimal control: linear quadratic methods*. Prentice-Hall information and system sciences series. Prentice Hall, 1989.

[8] R.A. Horn and C.R. Johnson. *Matrix Analysis*. Matrix Analysis. Cambridge University Press, 2013.

[9] Isaac Kaminer, António M. Pascoal, Pramod P. Khargonekar, and Edward E. Coleman. A velocity algorithm for the implementation of gain-scheduled controllers. *Automatica*, 31(8):1185–1191, 1995.

[10] A. P. Aguiar and A. M. Pascoal. Dynamic positioning and way-point tracking of underactuated AUVs in the presence of ocean currents. *International Journal of Control*, 80(7):1092–1108, July 2007.

[11] A. Pascoal, I. Kaminer, and P. Oliveira. Navigation system design using time-varying complementary filters. *IEEE Transactions on Aerospace and Electronic Systems*, 36(4):1099–1114, 2000.

[12] R. Ghabcheloo, A. P. Aguiar, A. Pascoal, C. Silvestre, I. Kaminer, and J. Hespanha. Coordinated path-following control of multiple underactuated autonomous vehicles in the presence of communication failures. In *Proceedings of the 45th IEEE Conference on Decision and Control*, pages 4345–4350, 2006.